

# Dynamic DNA Methylation and Histone Modifications Contribute to Lentiviral Transgene Silencing in Murine Embryonic Carcinoma Cells

Jin He, Qing Yang, and Lung-Ji Chang\*

*Department of Molecular Genetics and Microbiology, Powell Gene Therapy Center and McKnight Brain Institute, University of Florida, Gainesville, Florida 32610-0266*

Received 31 March 2005/Accepted 26 July 2005

**Embryonic stem cells are subjected to a dynamic genome regulation during development. Here we report that the ectopic lentiviral transgenes are quickly silenced in murine embryonic carcinoma P19 cells. The silencing was correlated with CpG hypermethylation in the transgene promoter. Using high-resolution sodium bisulfite genome sequencing, we detected distinct DNA methylation kinetics in different proviral regions. DNase I sensitivity and chromatin immunoprecipitation assays revealed condensed chromatin structure and histone code switch during silencing. Longitudinal analysis of nonsilenced and silenced identical single-cell clones revealed that the silencing was coupled with CpG methylation in the promoter, as well as a global histone H3 deacetylation. Interestingly, the primer binding site and the packaging signal region appeared to serve as a DNA methylation initiation center which was rapidly hypermethylated regardless of transgene silencing and chromatin modifications. Analysis of cellular genes 45 to 50 kbp upstream and downstream of the integration site indicated that transcriptional activities of the flanking host genes were not affected. Genetic modifications of stem cells have great therapeutic potentials and our results picture a dynamic embryonic genome response to ectopic transgene integration that may have important implications in the future safety and efficacy modifications of stem cells.**

Stem cells are undifferentiated progenitor cells capable of both self-renewal and multiple lineage differentiation. Although until now only embryonic stem (ES) cells have been shown to give rise to differentiated cells of all three embryonic germ layers, it is known that certain adult stem cells such as hematopoietic stem cells (HSC) are also able to transdifferentiate into different cell types (12). The pluripotent potentials of both embryonic and adult stem cells provide the opportunities for replacement of damaged cells and tissues in diseased organs.

For some inherited and acquired diseases, it may be necessary to modify stem cells at the genetic level in order to correct genetic defects or provide normal gene functions. For this purpose, efficient and long-term gene delivery is required. Different viral vectors have been tested for their ability to target stem cells (14, 30, 31). Among these, the oncoretroviral vectors derived from Moloney murine leukemia virus (MoMLV) have been used widely as stem cell gene transfer tools because of their ability to integrate into host genome. However, the low transduction efficiency and rapid silencing of MoMLV vectors in stem cells have hampered the advance of stem cell-based gene therapy (8).

Different from oncoretroviral vectors, lentiviral vectors (LVs) are able to transduce both dividing and nondividing cells at high efficiency. This makes LVs attractive for stem cell gene transfer. Previous studies have demonstrated that human immunodeficiency virus type 1 (HIV-1)-derived LVs are able to

transduce both embryonic and adult stem cells efficiently (7, 30). Several studies using lentiviral modification of stem cells for therapeutic purpose have reported promising results in animal models (10, 17, 23).

Whereas oncoretroviral vectors tend to favor integration near promoter regions, LVs tend to integrate into intra- or intergenic regions in the host genome (26). The chromatin environment surrounding the integration site may inevitably influence both the transgene and the host gene expression. Such chromatin effects on transgene expression have been well characterized with oncoretroviral gene transfer. It is generally agreed that both *cis* elements of the oncoretrovirus and *trans*-acting factors in the host cells contribute to the transcriptional repression (22). Whether LVs are also subjected to transgene silencing, however, is still controversial, and the underlying molecular mechanisms remain elusive (9, 16, 24, 25).

The murine embryonic carcinoma (EC) P19 cells are derived from teratocarcinomas induced in C3H/HC mice and are one of the best-characterized pluripotent embryonic cell lines (18). These cells are capable of differentiating into a variety of tissues when injected into normal embryos (19). It has been shown that the mechanisms of oncoretroviral transgene silencing in P19 cells also play roles in silencing events occurred in normal preimplantation embryos and other types of precursor cells (3, 27). Thus, both EC and ES cells may operate a similar gene silencing machinery.

Using the P19 cells as a model system, we characterized an interesting silencing event of the HIV-1-based self-inactivating (SIN) LVs. We found that SIN LVs with different internal promoters exhibited rapid transgene silencing after transduction of P19 cells. The transgene silencing was correlated with DNA methylation in the internal promoter. High-resolution

\* Corresponding author. Mailing address: Department of Molecular Genetics and Microbiology, Powell Gene Therapy Center and McKnight Brain Institute, University of Florida, 1600 SW Archer Rd., ARB, R1-252, Box 100266, Gainesville, FL 32610-0266. Phone: (352) 392-3315. Fax: (352) 392-3133. E-mail: lchang@mgm.ufl.edu.

analysis of DNA methylation in three CpG islands in the provirus revealed that the LV silencing was coupled with a wave of differential CpG methylation kinetics across the proviral loci. We further characterized the chromatin modification status during silencing and detected changes in chromatin structure and histone code in nonsilenced and silenced pooled and single-cell clones. A model for the epigenetic modifications of integrated LVs and the flanking gene expression profile in EC cells is presented.

## MATERIALS AND METHODS

**Cell culture and chemical treatment.** Murine EC cell line P19 was maintained in minimal essential alpha medium (Gibco-BRL) supplemented with 10% fetal bovine serum and 100 U of penicillin-streptomycin/ml. 5-Aza-2'-deoxycytidine (5-azaC; Sigma-Aldrich) was used at concentrations of 0, 2.5, 5.0, and 10.0  $\mu$ M to treat transgene-silenced cell clones for 48 h.

**Lentiviral vector production and titration.** LVs were generated by DNA cotransfection into 293T cells and the virus was concentrated by centrifugation and filtration, and the titer of the nlacZ virus was determined on TE671 cells by  $\beta$ -galactosidase enzyme assay as described previously (33). The chicken beta-actin promoter (CBA) promoter was a gift of Terry Flotte (University of Florida).

**Lentiviral transduction and single-cell cloning.** To obtain individual cell clones with a single copy of integrated provirus,  $10^5$  P19 cells were transduced with lentiviral EF1 $\alpha$ -nlacZ vector (LV-EZ) at multiplicity of infection (MOI) of 0.1 in the presence of Polybrene (8  $\mu$ g/ml; Sigma-Aldrich). At 3 days after transduction, the P19 cells were serially diluted and split into 96-well plate at 0.3 cell/well. The cells were duplicated into two plates after expansion. The LacZ-positive cells were identified by  $\beta$ -galactosidase staining. The nuclear LacZ-positive cell clones were further propagated and diluted into 10-cm dishes at ca. 100 cells/dish and, after expansion, the single-cell clones were picked and cloned.

**Southern and Northern analyses.** Genomic DNA was harvested by using Wizard Genomic DNA Purification Kit (Promega) for Southern analysis. A total of 15  $\mu$ g of genomic DNA was digested by selected restriction enzymes and separated by electrophoresis on 1.0% agarose gel. DNA was transferred to nylon membrane and hybridized with [<sup>32</sup>P]dCTP-labeled probes as described previously (33). For Northern analysis, total RNA was harvested by using Tri-reagent (Molecular Research Center, Inc.), and 15  $\mu$ g of total RNA was separated by electrophoresis on 1.6% formaldehyde denaturing agarose gel. The RNA was transferred to nylon membrane and hybridized with [<sup>32</sup>P]dCTP-labeled probes as described previously (33).

**Provirus integration site cloning.** A total 15  $\mu$ g of genomic DNA was cut by NlaIII or SphI and separated by 1% agarose gel electrophoresis. The size of the DNA fragment containing integration junction was estimated according to the Southern blotting result. The DNA was cut from the gel and purified by using QiaQuick gel purification kit (QIAGEN) and self-ligated. Circularized DNA was amplified with outwardly directed primers in conserved regions of the HIV-1 LTR and *gag*: outer long terminal repeat (LTR) primer, 5'-GGA TCT CTA GTT ACC AGA GTC ACA-3', nucleotides [nt] 574 to 600 in the LTR; and outer *gag* primer, 5'-CCA TCC CTT CAG ACA GGA TCA GA-3', nt 982 to 1007 in *gag*. This amplified the junction between the 5' end of the viral genome and the host cell DNA. PCR conditions were as follows. DNA was denatured at 94°C for 3 min, followed by 30 cycles of amplification at 94°C for 30 s, 55°C for 30 s, and 72°C for 2 min. A final extension was carried out for 10 min at 72°C. A second PCR was carried out with the same cycling parameters and a nested set of outwardly directed primers: HIV-1-specific inner LTR primer, 5'-CAG AGA GCT CCC AGG CTC AGA TC-3', nt 474 to 499 in the LTR; and inner *gag* primer, 5'-AGA TCT CCC TAT AGT GCA GAA CCT CCA GGG GC-3', nt 1185 to 1210 in *gag*. The PCR product was cloned into pST-Blue plasmid (Novagen) and sequenced. The sequence was BLAST searched against the NCBI mouse genome database.

**DNase I sensitivity assay.** P19 cells ( $5 \times 10^6$ , LacZ-positive or -negative clones) were treated with trypsin, pelleted, and washed with culture medium twice. The cells were equally distributed into five aliquots and treated with 2.5 ml of NP-40 buffer (300 mM sucrose, 15 mM Tris-HCl [pH 7.5], 60 mM KCl, 15 mM NaCl, 5 mM MgCl<sub>2</sub>, supplemented with 0.5 mM  $\beta$ -mercaptoethanol, and 0.2% NP-40 before use) containing DNase I at concentrations of 0, 50, 100, 150, 200 U/ml at room temperature for exactly 4 min; after that 0.5 ml of 6 $\times$  lysis buffer (6% sodium dodecyl sulfate [SDS], 300 mM Tris-HCl [pH 8.0], and 120 mM EDTA) was added to quench

the reaction. The lysates were then treated with 40  $\mu$ l of proteinase K (20 mg/ml) at room temperature overnight. The genomic DNA was purified after phenol-chloroform extraction, 15  $\mu$ g of genomic DNA from each sample was digested by HindIII, and the Southern blot was hybridized with <sup>32</sup>P-labeled EF1 $\alpha$  DNA probe or control murine  $\beta$ -actin promoter probe as described in the figure legends.

**Chromatin immunoprecipitation (ChIP) assay.** We plated  $10^7$  cells in a 10-cm dish and treated the cells with 1% formaldehyde (Fisher Scientific) for 10 min and 0.125 M glycine for 5 min to cross-link the DNA and proteins. The cells were then lysed in hypotonic buffer (10 mM HEPES-KOH [pH 7.8], 10 mM KCl, and 1.5 mM MgCl<sub>2</sub> in 1 $\times$  protease cocktail [1 mM phenylmethylsulfonyl fluoride, 1 mg of aprotinin/ml, and 1 mg of pepstatin A/ml]) and nuclei lysis buffer (1% SDS, 50 mM Tris-HCl [pH 8.0], and 10 mM EDTA in 1 $\times$  protease cocktail). The genomic DNA was fragmented by sonication, and 25  $\mu$ g of DNA was precleared by incubation with salmon sperm DNA-protein G agarose slurry for 30 min at 4°C. The supernatant was incubated with 2  $\mu$ g of rabbit anti-acetyl H3 antibody (Upstate Biotech, Inc.), rabbit anti-H3 diMeK4 (ab7766; Abcam, Inc., Cambridge, MA), or rabbit anti-H3 diMeK9 (ab7312; Abcam) in immunoprecipitation buffer (0.01% SDS, 20 mM Tris-HCl [pH 8.0], 1.1% Triton X-100, 167 mM NaCl, and 1.2 mM EDTA in 1 $\times$  protease cocktail) at 4°C overnight. To pull down antibody-DNA-protein, 60  $\mu$ l of salmon sperm DNA-protein G agarose slurry was added, followed by incubation for 1 h. The agarose beads were serially washed with wash buffer I (0.1% SDS, 1% Triton X-100, 2 mM EDTA, 20 mM Tris-HCl [pH 8.0], 150 mM NaCl), wash buffer II (0.1% SDS, 1% Triton X-100, 2 mM EDTA, 20 mM Tris-HCl [pH 8.0], 500 mM NaCl), wash buffer III (250 mM LiCl, 1% NP-40, 1% sodium deoxycholate, 1 mM EDTA, 10 mM Tris-HCl [pH 8.0]) and TE buffer (10 mM Tris-HCl [pH 8.0], 1 mM EDTA). The DNA-protein was eluted by incubation with elution buffer (1% SDS, 100 mM NaHCO<sub>3</sub>), and the eluted mix was incubated at 65°C for 6 to 8 h to reverse the DNA-protein cross-link. The DNA was isolated by phenol-chloroform extraction and ethanol precipitated, the DNA pellet was dissolved in 100  $\mu$ l of H<sub>2</sub>O, and 5  $\mu$ l of each sample was used for PCR amplification. The primers used for PCR were as follows: EF1 $\alpha$  promoter, 5'-TAA GCC AGC AAT GGT AGA GG-3' and 5'-ACA CGA CAT CAC TTT CCC AG-3'; murine  $\beta$ -actin promoter, 5'-ATG CTG CAC TGT GCG GCG AG-3' and 5'-TGG CTG CAA AGA GTC TAC ACG-3'; lacZ 1, 5'-AGG ATA TGT GGC GGA TGA GC-3' and 5'-TGC TTC AAT CAG CGT GCC GTC-3'; lacZ 2, 5'-GCT TTC GCT ACC TGG AGA G-3' and 5'-ATG ACG GAA CAG GTA TTC GCT GG; lacZ 3, 5'-TGA AGT GGC GAG CGA TAC AC-3' and 5'-GAA ACC GTC GAT ATT CAG CC-3'; provirus 1, 5'-ATG GGT CCG AGA TCT TCA GAC-3' and 5'-ACA GCC AGG ATT CTT GCC-3'; and provirus 2, 5'-AGA CAA ATA CTG GGA CAG C-3' and 5'-TCT GGG CTG AAA GCC TTC TC-3'.

**Sodium bisulfite genome sequencing.** The genomic DNA (2  $\mu$ g) was digested with an appropriate restriction enzyme and purified by MinElute Reaction Cleanup Kit (QIAGEN). The purified DNA was chemically treated and cleaned by using a EZ DNA methylation kit (Zymo Research, Inc.). The recovered bisulfite-treated sample was subjected to PCR with HotStarTaq polymerase in the provided buffer (QIAGEN) under the following conditions: 94°C for 5 min, followed by 35 cycles of 94°C for 45 s, 55°C for 30 s, and 72°C for 60s, with a final extension at 72°C for 10 min. The PCR primers were as follows: 5' PBS+ $\psi$ , 5'-TAG TGT GGA AAA TTT TTA GTA GTG G-3'; 3' PBS+ $\psi$ , 5'-AAT TTA TAG TAT TTC TTC CCC CTA ACC-3'; 5' EF1 $\alpha$  promoter, 5'-TAG TAA TGG TAG AGG GAA GAT TTT GTA-3'; 3' EF1 $\alpha$  promoter, 5'-ACT CTT CTC CAC CTC AAT AAT AAC-3'; 5' EF1 $\alpha$  intron, 5'-TTG TTG TAGGGA GTT TAA AAT GGA G-3'; and 3' EF1 $\alpha$  intron, 5'-CCA CCC ACT CAA TAT AAA AAA CTC-3'. PCR products were gel purified by using QIAGEN's QiaQuick kit, ligated into the pST-Blue plasmid (Novagen), and transformed into competent bacterial cells. Plasmids from individual colonies were subjected to automated sequencing with the ABI Prism BigDye terminator cycle sequencing ready reaction kit with AmpliTaq DNA polymerase. At least 10 plasmid clones were sequenced from the PCR products generated by each primer set.

## RESULTS

**Silencing of lentiviral transgenes in murine EC cells.** P19 cells were transduced with a SIN LV carrying a nuclear  $\beta$ -galactosidase (LacZ) reporter gene driven by an internal human elongation factor 1 $\alpha$  promoter (EF1 $\alpha$ ) (33). The P19 cells were infected at an MOI of 5, and the transgene expression was monitored by  $\beta$ -galactosidase staining kinetically. We found that the peak LacZ expression occurred at day 2, and the population of LacZ-positive cells quickly decreased from 70 to

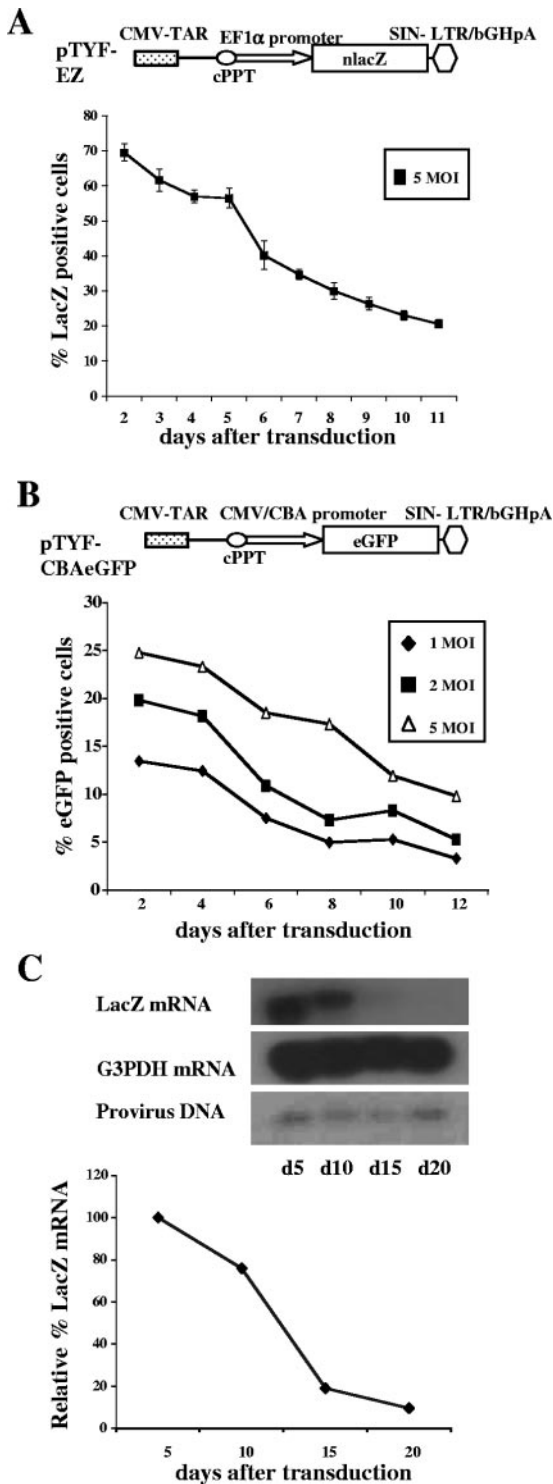


FIG. 1. Lentiviral transgene silencing in murine EC cells. Murine EC P19 cells were transduced by SIN LVs carrying different promoters and reporter genes, and the expression kinetics of the LVs were monitored by  $\beta$ -galactosidase enzyme assay (nlacZ) or flow cytometry (eGFP). (A) LV nlacZ transduction at 5 MOI. (B) LV eGFP transduction at MOIs of 1, 2, and 5. (C) Kinetics of LV transgene expression and copy number of the proviral DNA. The LV lacZ mRNA was analyzed by Northern blotting and the proviral DNA by Southern blotting at 5, 10, 15 and 20 days after transduction. The signals were quantified by using a phosphorimager as follows:

~25% in less than 2 weeks (Fig. 1A).<sup>1</sup> This effect was independent of the internal promoter type or the transgene because P19 cells transduced with LV expressing enhanced green fluorescence protein (eGFP) driven by human cytomegalovirus (CMV)-CBA exhibited the same effect. As illustrated in Fig. 1B, P19 cells were infected at different MOIs (1, 2, and 5), and the eGFP expression was monitored by flow cytometry analysis.

To exclude the possible transient effects due to pseudotransduction or unintegrated provirus, we monitored the integrated provirus copy number and the transgene transcription at days 5, 10, 15, and 20 after transduction by Southern and Northern analysis (Fig. 1C). Consistent with the expression kinetics, we noted that the transgene mRNA level decreased quickly in 10 to 15 days; however, the provirus DNA copy number remained the same. The silencing of transgene was most prominent between 10 and 15 days postinfection (dpi). This was not due to LV cytotoxicity to P19 cells because there was no obvious cell death after infection. These results demonstrated that LV transgenes were subjected to transcriptional silencing in P19 cells at a very early stage after gene transfer.

**Silencing of lentiviral transgene was associated with CpG hypermethylation of the internal promoter.** Transcriptional silencing is often caused by epigenetic changes including cytosine methylation at CpG dinucleotides and chromatin modifications. To gain insight into the mechanisms leading to LV transgene silencing, we treated the silenced P19 cells with DNA methyltransferase (DNMT) inhibitor 5-azacytidine C (5-azaC) at different concentrations for 48 h and assayed for the lentiviral LacZ expression. We found that 5-azaC was able to reactivate nuclear LacZ expression in a dosage-dependent manner (Fig. 2A); interestingly, the potential of transgene reactivation by this DNMT inhibitor appeared to diminish over time (not shown). The 5-azaC effect suggested that DNA methylation played some roles in LV silencing in the EC cells.

To determine whether DNA methylation in the EF1 $\alpha$  promoter region contributed to transgene silencing, DNA methylation analysis was performed by using pooled transduced P19 cells at early (5 dpi) and late (25 dpi) passages when the LV lacZ became silenced (Fig. 2B). The genomic DNA was harvested from cells of the two time points and digested with methylation-sensitive restriction enzyme AgeI. The digestion produced an AgeI-uncleaved 1.5-kb band (methylated) and an AgeI-cleaved 1.09-kb band (unmethylated) that were resolved by Southern analysis (Fig. 2C). Quantitative analysis of the AgeI sensitivity (uncleaved/cleaved signal ratios) illustrated that the silencing was correlated with increased methylation in the EF1 $\alpha$  promoter (Fig. 2D).

**Dynamic CpG island methylation in the provirus during transgene silencing.** To determine whether there were negative *cis* elements in the LV-EZ provirus that might have contributed to the transgene silencing, CpG islands in the provirus were

percent lacZ mRNA = (intensity of lacZ mRNA/intensity of G3PDH [glyceraldehyde-3-phosphate dehydrogenase] mRNA)/(day 5 intensity of lacZ mRNA/day 5 intensity of G3PDH mRNA)  $\times$  100, with the relative intensity of d5 mRNA arbitrarily set as 100%.

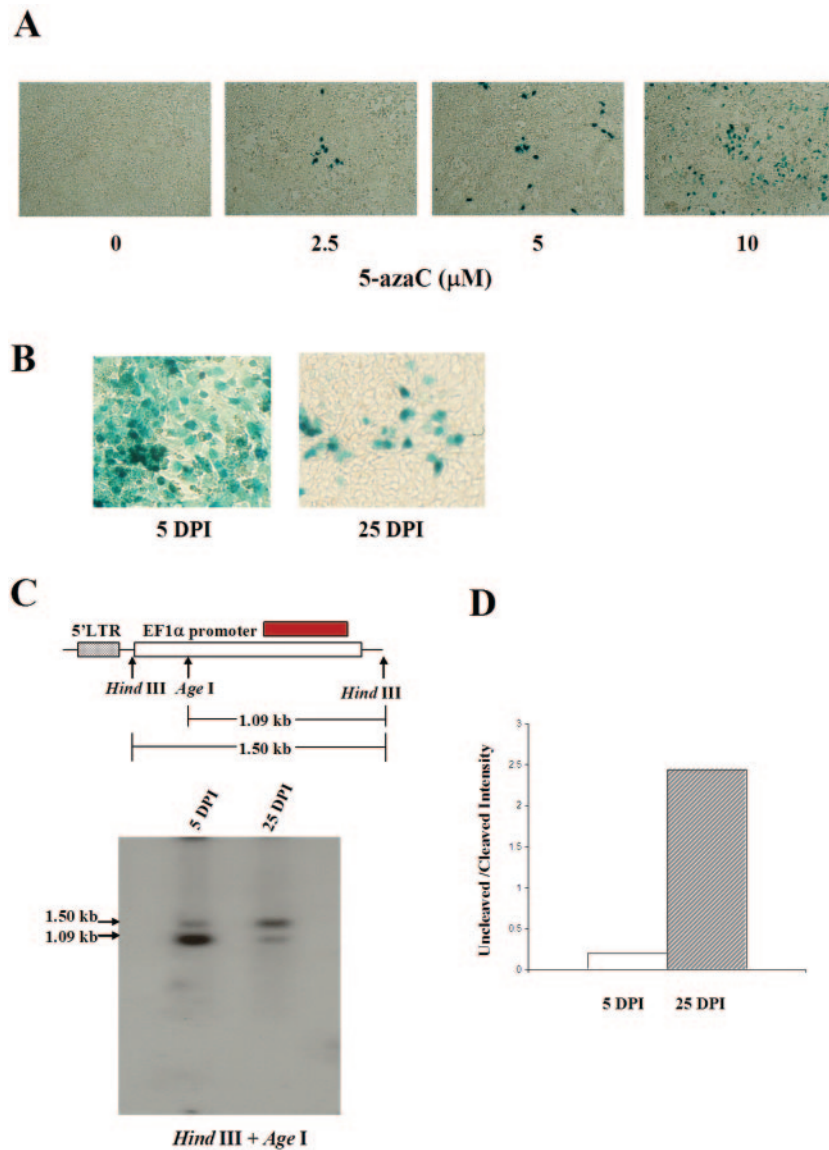


FIG. 2. Correlation of DNA methylation with LV transgene silencing. (A) Reactivation of silenced LV in P19 cells by 5-azaC treatment. The LV lacZ expression in silenced P19 cells (5D11) was reactivated after exposure to 5-azaC at 0.0, 2.5, 5.0, and 10  $\mu\text{M}$  for 48 h. (B) Illustration of LV lacZ silencing in transduced P19 cells. The P19 cells were transduced by pTYF-EZ LV and stained for lacZ expression on day 5 (5 dpi) and day 25 (25 dpi). (C) Analysis of CpG methylation in the internal EF1 $\alpha$  promoter region in the transduced P19 cells in early (day 5) and late (day 25) time points. The genomic DNA was harvested and digested with HindIII and a CpG methylation-sensitive enzyme, AgeI, followed by Southern analysis. (D) Relative CpG methylation level in the EF1 $\alpha$  promoter in the provirus at 5 dpi and 25 dpi: degree of CpG methylation = intensity of uncleaved band/intensity of cleaved band.

identified by using CpGplot/CpGReport software. We found three CpG-rich regions (CpG%, >50%; Observed CpG/Expected CpG, >60%; length, >100 nt) in the provirus: the primer binding site plus the packing signal region (PBS+ $\psi$ , 613 to 829 nt of pNL4-3, AF324493), the internal EF1 $\alpha$  promoter (159 to 880 nt of human EF1 $\alpha$ , J04617), and the EF1 $\alpha$  intron (929 to 1,396 nt of human EF1 $\alpha$ , J04617) (Fig. 3A). To determine the CpG methylation status in these regions during LV transgene silencing, we analyzed the process of CpG methylation by a time kinetic study. The genomic DNA of infected P19 cells was harvested at four different time points after LV infection and treated by sodium bisulfite and followed by

PCR amplification, DNA cloning, and sequencing with specific primers (Fig. 3B, each row of circles represents one amplified fragment). We found that the PBS+ $\psi$  region was heavily methylated (75%) as early as 5 dpi even when the transgene expression level was still high; it reached saturation (100%) by 15 dpi. In contrast, CpG methylation in the EF1 $\alpha$  promoter region progressed gradually, from 42% at 5 dpi to near 100% by D15, a finding consistent with the rate of transgene silencing. The EF1 $\alpha$  intron region was methylated much more slowly, from 30% at 5 dpi to 84% at 20 dpi (Fig. 3C). These results demonstrated that all three CpG-rich regions in the provirus were subjected to a dynamic process of DNA methylation,

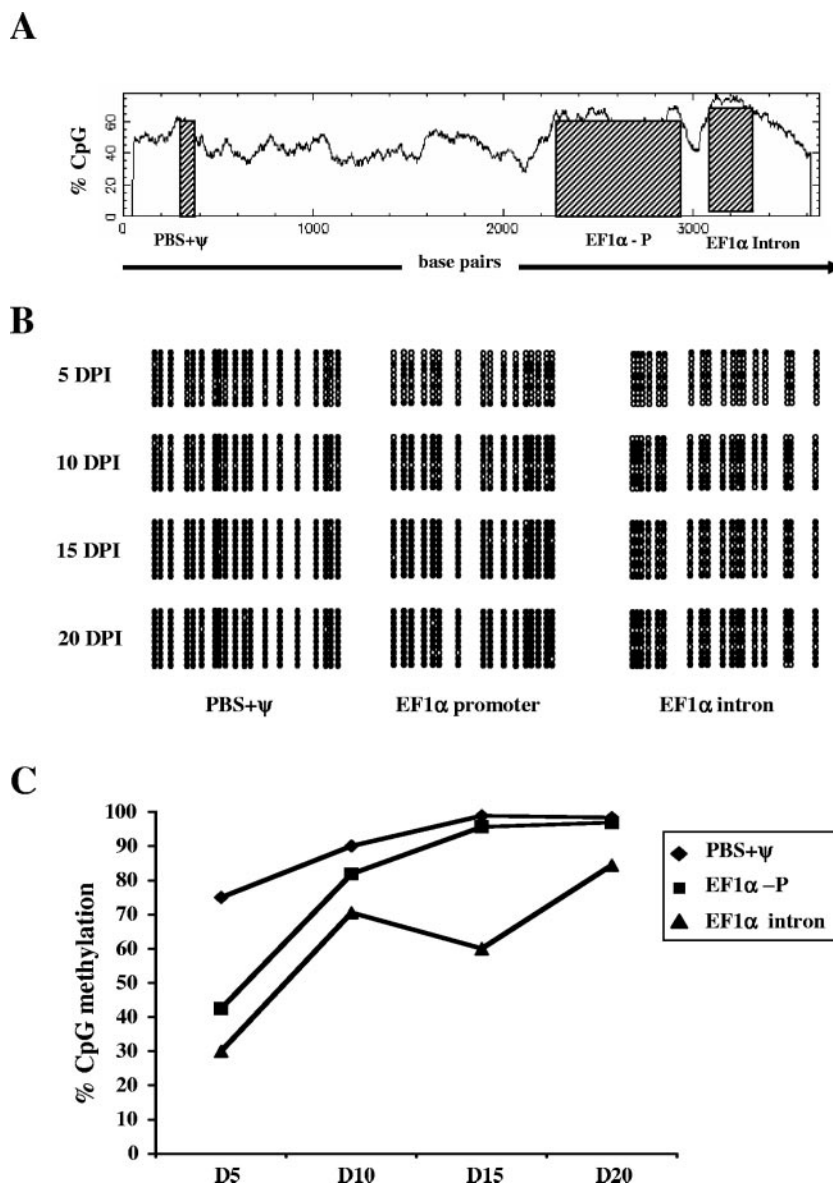


FIG. 3. Kinetics of hypermethylation of CpG islands in the integrated provirus. (A) Mapping of CpG islands in the provirus. The CpG-rich regions (%CpG, >50%; observed CpG/expected CpG, >60%; length, >100 nt) in the pTYF EZ LV were mapped to three regions—the PBS+Ψ, EF1α promoter (EF1α-P), and EF1α intron regions—by using the CpGplot/CpGReport software. (B) CpG methylation analysis by bisulfite genome PCR sequencing. The P19 genomic DNA was harvested at 5, 10, 15, and 20 dpi; treated with bisulfite; PCR amplified with primers specific to the three CpG islands; and individually cloned and sequenced. Filled and closed circles correspond to methylated and unmethylated CpG residues, respectively. The distribution of the CpG sites shown is proportional to their relative locations in the pTYF-EZ provirus. (C) Illustration of CpG methylation kinetics in the integrated provirus in P19 cells, calculated as follows: percent CpG methylation = (methylated CpG of all sequenced clones/total CpG of all sequenced clones) × 100.

with rapid methylation in the PBS+ψ region independent of transgene silencing, and methylation in the EF1α promoter region closely correlated with transgene silencing.

**Positional effects of integrated provirus in transcriptionally active versus nonactive loci.** To characterize possible local chromatin modifications during lentiviral transgene silencing, we investigated cell clones containing single integrated provirus with defined chromatin environment. To generate P19 cell clones with single proviral integration, we transduced P19 cells with LV-EZ at a low MOI (0.1) for 3 days and serially diluted

into a 96-well plate at a density of 0.3 cell/well. The frequency of the LacZ-positive cell clones was very low, ca. 1%, during the 2- to 3-week expansion. This low frequency further supported that the lentiviral transgene was rapidly silenced in P19 cells. These rare positive cells were individually cloned and expanded. Interestingly, we found that the LacZ-positive cell clones were quickly diverted into three different phenotypes after a few passages: “Mixed” (mixed LacZ positive and negative), “Positive” (all LacZ positive) and “Negative” (all LacZ negative) (Fig. 4A and Fig. 5). Southern analysis of

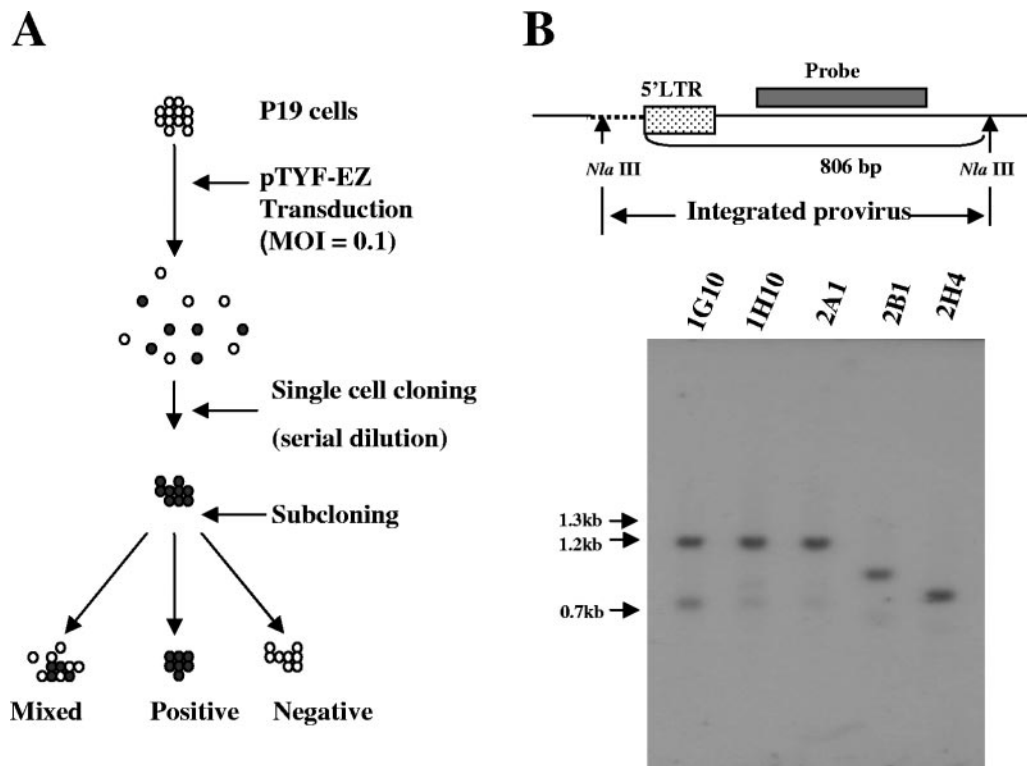


FIG. 4. Characterization of LV silencing in single-cell clones. (A) Schematic illustration of P19 single-cell cloning. P19 cells were transduced with pTYF-EZ LV at an MOI of 0.1, and single-cell clones were isolated by serial dilution and analyzed by  $\beta$ -galactosidase enzyme staining. The positive clones were passed and subcloned, and this led to three types of subcloned cells: Mixed (partial silenced), Positive (all lacZ positive), and Negative (all silenced). (B) Southern analysis of provirus copy number in the single-cell clones. The genomic DNA of five different single-cell clones was digested by *Nla*III, and analyzed by Southern analysis. The blot was hybridized to a [ $^{32}$ P]dCTP-labeled probe as shown in the diagram.

genomic DNA from five different clones showed that all of them had a single copy of integrated provirus (Fig. 4B). To determine whether the different phenotypes derived from a single-cell clone (5D11, Fig. 5A) was due to the loss of the integrated provirus, genomic DNA of the Mixed, Positive, and Negative subclones was harvested and analyzed. The result showed that all of them still contained the same amount of integrated provirus (Fig. 5B).

The integration sites of several transduced P19 cell clones were characterized by a ligation and inverse PCR method which amplifies DNA at the junction of the provirus and the host genome. The host DNA sequences were BLAST searched against NCBI mouse genome database and the results demonstrated that LV integrated at intragenic, untranscribed, or endogenous retrovirus location as summarized in Table 1. We propagated all of these single-cell clones and analyzed transgene expression and silencing to determine whether there was any correlation with the site of integration. The expression analysis revealed that high expression appeared to correspond well with integration at actively transcribed loci (e.g., 2B1 and 5D11), whereas low expression or silencing correlated with integration into inert endogenous retrovirus or inactive genome loci.

**The silenced LV promoter displayed a condensed chromatin structure with altered histone code.** In addition to promoter hypermethylation, transcriptional silencing may also involve chromatin modifications. To examine this possibility, we fo-

cused our study on proviral insertion into actively transcribed loci that likely have an open chromatin structure. The provirus of the 5D11 clone integrates at the sixth intron of the paraspeckle protein gene which is actively transcribed (5). We treated both Positive and Negative 5D11 cells with DNase I in situ and followed by restriction enzyme digestion and Southern blotting. This allows for the analysis of the integrity of the LV internal EF1 $\alpha$  promoter. The result revealed that the accessibility of DNase I to the EF1 $\alpha$  promoter was limited for the Negative (more intact DNA fragments) but not for the Positive 5D11 cells (degraded DNA fragments), indicating that the local chromatin structure surrounding the LV EF1 $\alpha$  promoter in the Positive 5D11 cells was relatively open but was more condensed and not accessible to DNase I in the Negative 5D11 cells (Fig. 6A, left panel). No such disparity was observed for the control house keeping gene  $\beta$ -actin promoter between Positive and Negative 5D11 cells (Fig. 6A, right panel).

An open chromatin structure is usually associated with active transcription and histone H3 acetylation. To determine whether LV silencing is accompanied by histone modifications, we performed a ChIP assay to analyze histone code in the EF1 $\alpha$  promoter region using both LacZ Positive and Negative P19 clones. Anti-acetyl H3 antibody was used to detect H3 acetylation. The result showed that anti-acetyl H3 antibody specifically enriched the EF1 $\alpha$  promoter DNA of the Positive cells but not the Negative cells; the  $\beta$ -actin promoter region, which had an open chromatin structure under all conditions,

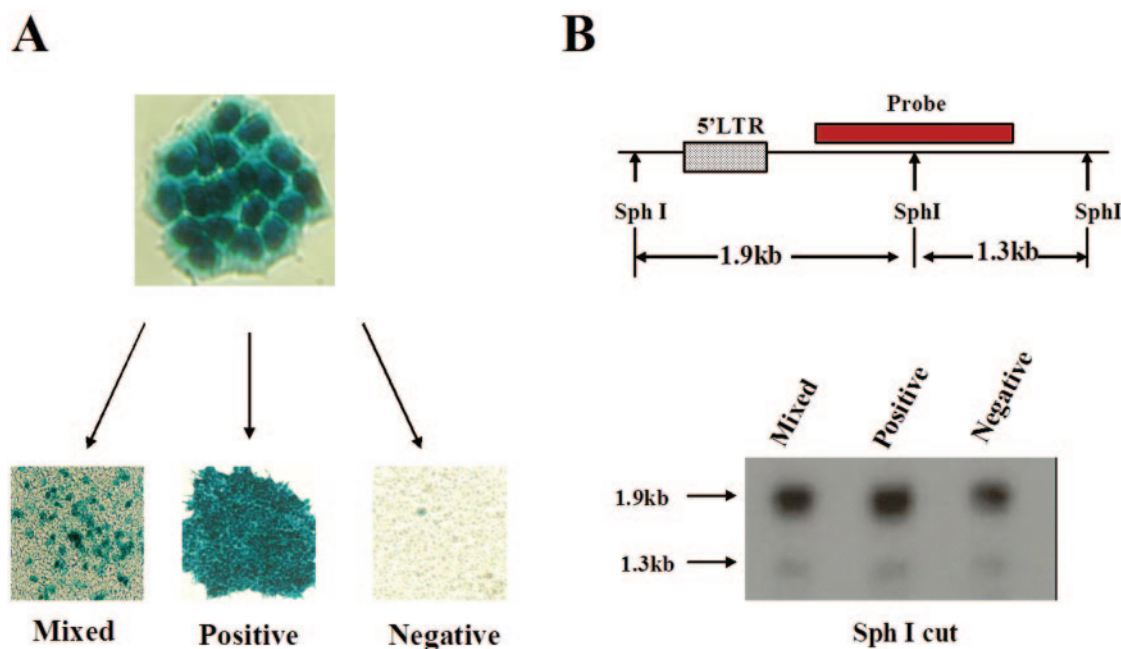


FIG. 5. Silencing due to loss of expression not loss of the transgene. (A) P19 single-cell clone 5D11 diverted from full expression to different expression phenotypes after several passages. (B) The different expression populations of 5D11 cells contained similar copies of provirus. The genomic DNA of Mixed, Positive, and Negative 5D11 cells were analyzed by Southern analysis; the DNA was digested by SphI and hybridized to the [<sup>32</sup>P]dCTP-labeled probe as illustrated.

was enriched by anti-acetyl H3 antibody in both Positive and Negative cells (Fig. 6B, upper panel). This suggested that the local H3 became deacetylated after transgene silencing, a finding consistent with the chromatin condensation observation.

In eukaryotic cells, methylation of lysine 4 at the H3 tail was a typical histone code for euchromatin, whereas methylation of lysine 9 at the H3 tail was a marker for heterochromatin (29). To determine whether there was histone code difference after transgene silencing, both anti-H3 dimethyl lysine 4 (diMeK4) and anti-H3 dimethyl lysine 9 (diMeK9) antibodies were used in the ChIP assay. The result clearly illustrated that the LV EF1 $\alpha$  promoter DNA was specifically enriched by anti-diMeK4 antibody, a finding consistent with the euchromatin pattern, in the Positive cells, in contrast to the enrichment with anti-diMeK9 antibody in the Negative cells, a finding consistent with the heterochromatin pattern (Fig. 6B, middle and

bottom panels). No such dichotomy was observed for the control  $\beta$ -actin promoter in these two types of cells.

**Dynamic changes of CpG methylation and chromatin modifications during lentiviral transgene silencing.** The epigenetic changes including DNA methylation and chromatin modifications are a dynamic process that may spread into neighboring regions. To characterize CpG methylation kinetics during LV silencing, we determined the methylation patterns in the PBS+ $\psi$ , EF1 $\alpha$  promoter, and the EF1 $\alpha$  intron regions by sodium bisulfite sequencing using both Positive and Negative cells of the 5D11 clone (Fig. 7). Interestingly, we found that the PBS+ $\psi$  region was hypermethylated (>95%) in both Positive and Negative cells regardless of the transgene expression status (Fig. 7B, left panel). However, a marked difference in CpG methylation was observed in the EF1 $\alpha$  promoter and intron regions between Positive and Negative cells; the two sites were unmethylated in the Positive cells but completely methylated in the Negative cells (Fig. 7B, middle and right panels).

To expand our analysis, we examine the chromatin modifications beyond the EF1 $\alpha$  region in both Positive and Negative 5D11 cells. The status of H3 acetylation/deacetylation was determined across the entire provirus in six sites (1 kb apart, Fig. 7A, R1 to R6) using anti-acetyl H3 antibody and ChIP assay. We found that H3 deacetylation was not only restricted to the methylated regions in the Negative cells but also spread to the entire 7-kb provirus; in contrast, no H3 deacetylation was observed in the Positive cells (Fig. 7C). This revealed that in the silenced cells the chromatin of the entire provirus had been modified to heterochromatin-like structure although the CpG methylation appeared to be restricted at certain locations. All of these findings suggest that LV silencing takes place when the EF1 $\alpha$  promoter becomes hypermethylated, and

TABLE 1. Analysis of LV integration sites and expression of P19 single-cell clones<sup>a</sup>

Clone	Chromosome/locus <sup>b</sup>	LacZ expression <sup>c</sup>	Silencing rate <sup>d</sup>
1G10	NA/junction of two ERVK	+	+++
1H10	8/nontranscribed region	+	+++
2B1	2/16th intron, 6030446I19 gene	+++	++
2H4	12 or X/NA	++	+
5D11	14/6th intron, paraspeckle gene	+++	+

<sup>a</sup> P19 cells were transduced with LV-EZ at a low MOI, single proviral integration clones were isolated, and the integration sites were cloned and sequenced. The expression and silencing rates were determined and arbitrarily set as indicated.

<sup>b</sup> NA, not available; ERVK, endogenous retrovirus type K.

<sup>c</sup> +, Light blue; ++, medium blue; +++, strong blue.

<sup>d</sup> +++, >75%; ++, 25 to 75%; +, <25%. LacZ was silenced in 1 month.

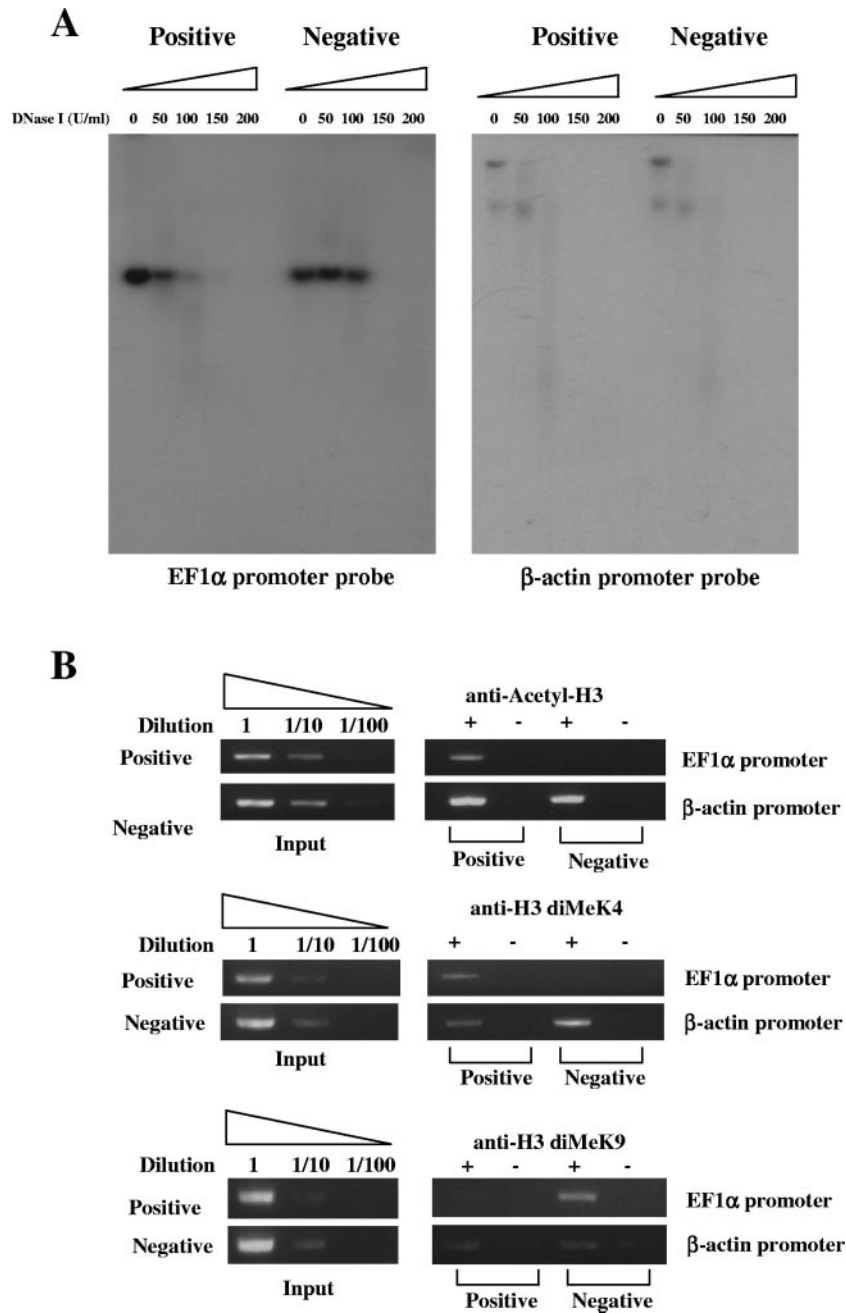


FIG. 6. Chromatin analysis of integrated provirus. (A) DNase I sensitivity assay. The silenced (Negative) and nonsilenced (Positive) 5D11 cells were treated with different concentrations of DNase I as indicated, and the genomic DNA (15  $\mu$ g) was harvested, digested with HindIII, and analyzed by Southern blotting with EF1 $\alpha$  or  $\beta$ -actin promoter probe. (B) ChIP assay. The chromatin of both silenced and nonsilenced 5D11 cells were harvested and precipitated with anti-acetyl-H3 antibody, anti-diMeK4 antibody, or anti-diMeK9 antibody. The DNA was extracted and PCR amplified with specific primers for EF1 $\alpha$  promoter or  $\beta$ -actin promoter and analyzed by gel electrophoresis. The unprecipitated chromatin was amplified as control input DNA, and the antibody specific (+) and nonspecific (-) immunoprecipitated chromatin was amplified and illustrated.

the entire provirus is modified toward heterochromatin-like structure.

**The silencing of the integrated provirus did not spread to the neighboring host genes.** The ChIP analysis revealed that the entire provirus was gradually modified, suggesting that it was possible that the chromatin modification might also spread to the neighboring host genes and alter their expression. To examine this possibility, we analyzed the flanking host gene expression

using both Positive and Negative 5D11 cells, in comparison with untransduced P19 cells. The provirus in 5D11 cells was integrated into the sixth intron of paraspeckle protein gene at chromosome 14 in the forward transcriptional orientation and flanked by 4930548G07RiK and MGC38922, located 45 kbp upstream and 50 kbp downstream from the integration site, respectively, as illustrated in Fig. 8A. We examined the transcriptional activities of these three genes by Northern analysis with RNA harvested



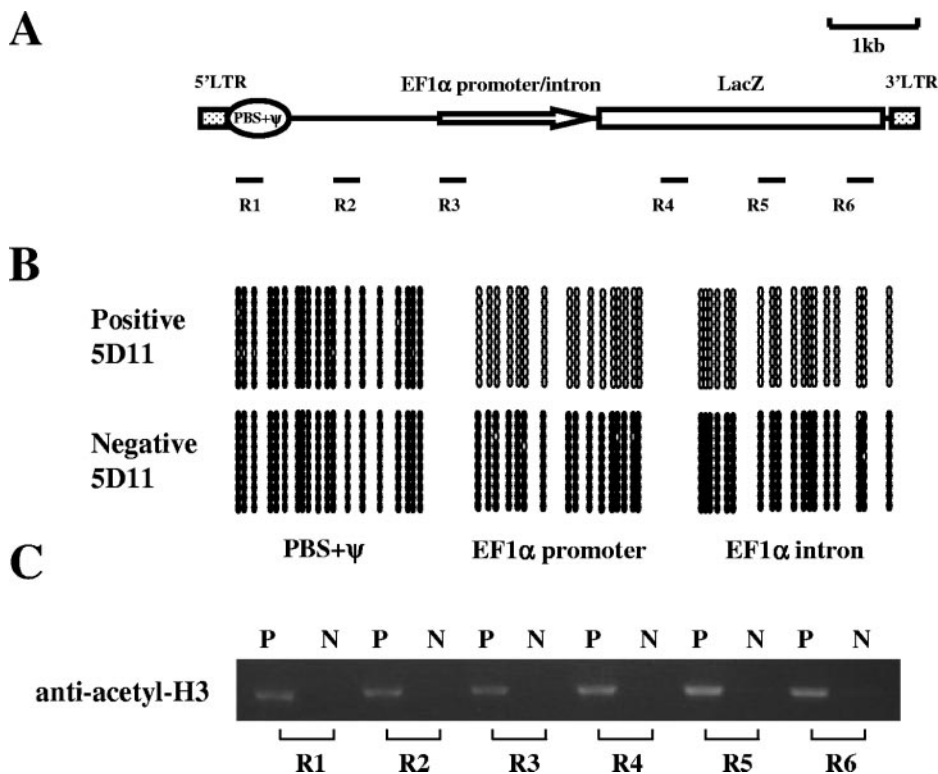


FIG. 7. Comparison of CpG methylation and chromatin modifications between silenced and nonsilenced 5D11 cells. (A) Schematic illustration of LV-EZ provirus and six regions analyzed by anti-acetyl-H3 antibody ChIP assay. (B) Bisulfite genome sequencing of the three CpG islands in Positive (nonsilenced) and Negative (Silenced) 5D11 cells. The filled circles correspond to methylated CpG, and open ones correspond to unmethylated CpG. The spacing of the CpG sites is proportional to their actual locations in the specified CpG islands (PBS+ψ, EF1α promoter and intron). (C) Anti-acetyl-H3 antibody ChIP assay of histone code in the provirus. The chromatins of Positive (P) and Negative (N) 5D11 cells were immunoprecipitated and amplified with six pairs of primers specific to R1 to R6 across the entire provirus, and the products were analyzed by gel electrophoresis.

from control P19 cells, as well as nonsilenced (Positive) and silenced (Negative) 5D11 cells. The result showed that the transcription of the paraspeckle protein gene decreased by ca. 50% in both Positive and Negative 5D11 cells compared to the control P19 cells. However, the transcriptional activities of the flanking 4930548G07RiK and MGC38922 genes were similar in all three cell samples based on the quantity of the RNA signals on the Northern blots as illustrated in Fig. 8B and plotted in Fig. 8C.

**DISCUSSION**

Stem cells are ideal targets for gene therapy because of their self-renewal, proliferation, and pluripotent differentiation potential. For successful gene transfer into stem cells, suitable gene delivery vectors are necessary. The ideal vectors should be able to transduce cells efficiently and maintain transgene expression for long-term; at the same time, the host cell genome environment should not be disturbed. LVs are favored gene transfer tools because of their ability to transduce non-dividing cells and integrate into host genome. However, two questions remain with LV modification of stem cells: first, it is still controversial whether LVs are subjected to transgene silencing in stem cells; second, does LV integration affect flanking host gene functions?

Oncoretroviral vectors derived from MoMLV are subjected to transcriptional silencing in embryonic cells. In the MoMLV vectors, silencer elements have been localized in the LTR enhancer-promoter and the adjacent PBS; DNA methylation and/or chromatin modifications at or near these silencer elements have been shown to play a role in MoMLV silencing (22). HIV-1-derived LVs, however, seem to lack such silencer functions (9, 16, 24, 25).

Using SIN LVs carrying either human EF1α or CMV/CBA promoters, we demonstrated rapid transgene silencing in the murine EC cells. Kinetic analysis of proviral DNA and transgene expression showed that the decrease of transgene expression was due to transcriptional silencing and not deletion of the transgene. This result is consistent with previous reports that SIN LVs carrying internal promoters are silenced in other types of murine EC cell lines, HSC, and human embryonic cells, although the silencing rate varied in different studies (9, 16, 25).

DNA methylation and chromatin modifications are two main epigenetic changes contributing to transgene silencing. Two lines of evidence suggest that DNA methylation plays some roles in LV silencing in EC cells. First, DNA methyltransferase inhibitor 5-azaC partially reactivated transgene expression; second, DNA hypermethylation in EF1α promoter was detected along with the transgene silencing. It is interest-

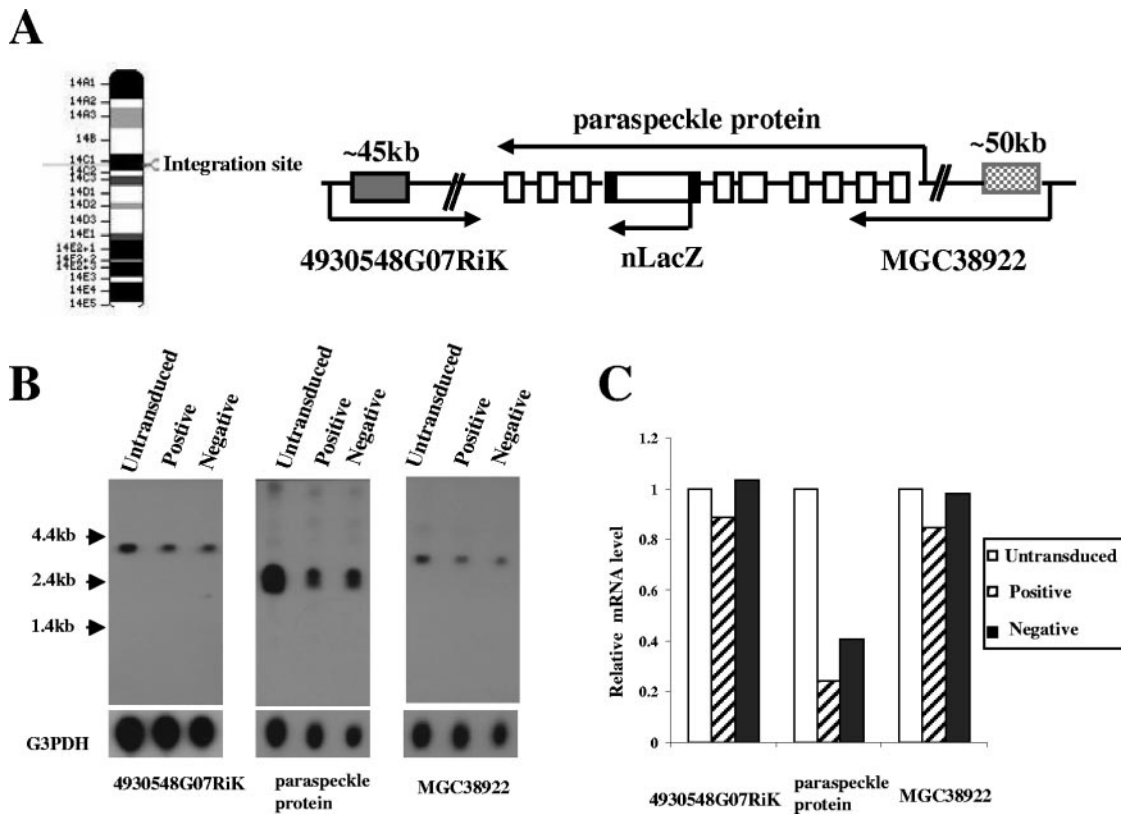


FIG. 8. Flanking cellular gene expression profile in silenced and nonsilenced LV transduced cells. (A) The configuration of integrated provirus in P19 5D11 cells. The LV was integrated into the sixth intron of paraspeckle protein gene on murine chromosome 14 flanked by 4930548G07RiK located approximately 45 kb upstream and MGC38922 located approximately 50 kb downstream from the integration site. (B) Northern analysis of host cell gene expression in untransduced and transduced (silenced and nonsilenced) cells. (C) Relative mRNA expression levels of the flanking cellular genes in untransduced and transduced cells. The RNA signals in the Northern blots were analyzed by using a phosphorimager and the RNA level in untransduced cells was arbitrarily set at 1.

ing that the degree of reactivation of the silenced transgene by 5-azaC gradually decreased over time, which suggests that other factors also play a role in permanent transgene silencing after the initial DNA hypermethylation-mediated silencing (1).

The silencing of the internal promoters (EF1 $\alpha$  and CBA) may involve some *cis*-regulatory elements. Kinetic analysis of DNA methylation in all three CpG-rich regions in the LV-EZ provirus by sodium bisulfite treatment and PCR sequencing demonstrated that different CpG regions displayed distinct methylation kinetics. The primer binding site and packaging signal regions were hypermethylated as early as 5 dpi even before transgene silencing. In contrast, CpG methylation in the EF1 $\alpha$  promoter and intron regions took place slowly and correlated well with the status of transgene silencing. These results suggest that transgene silencing is dominated or initiated by promoter methylation. This is also consistent with a previous report that transcriptional silencing was associated with DNA methylation of LTR promoter/enhancer in oncoretroviral vectors (2, 3, 6, 11).

There is a dichotomy in the methylation status of the CpG islands in the provirus. The PBS+ $\psi$  region is heavily methylated in both nonsilenced and silenced cells, whereas the internal EF1 $\alpha$  promoter and intron regions are methylated only in the silenced cells. Thus, CpG methylation in the PBS+ $\psi$  region is independent of transgene silencing. Transcriptional silencing

may occur after the "spread" of CpG methylation into the internal promoter region. Interestingly, the silencing of LV is similar to that of the mouse *aprt* (adenine phosphoribosyltransferase) gene which is shown to be gradually silenced in EC cells. In the latter case, a *cis* element located 1.3 kbp upstream of the *aprt* gene initiates a de novo methylation signal which further induces downstream promoter methylation, resulting in gene silencing (20, 28). We suspect that the PBS+ $\psi$  site may serve as a de novo "methylation center" in the lentiviral provirus and initiates the spread of DNA methylation. The signals that regulate PBS+ $\psi$  methylation and the factors that facilitate or block the spread of DNA methylation are not well understood and require further investigation.

In order to characterize genome modifications during LV silencing under a defined chromatin background, we chose a single-cell derived nonsilenced and silenced clone (5D11, with one proviral integration site) for detailed study. Although only one cell clone was extensively analyzed, multiple LV-transduced cell clones and pooled cells have shown similar silencing phenotypes (Fig. 1, 3, and 4 and Table 1; also, unpublished data). Using a DNase I sensitivity assay, we noted that the chromatin in the hypermethylated and silenced LV promoter region became condensed and resistant to DNase I digestion. The ChIP assay confirmed that the histone H3 was deacetylated and the histone code was switched from the euchromatin

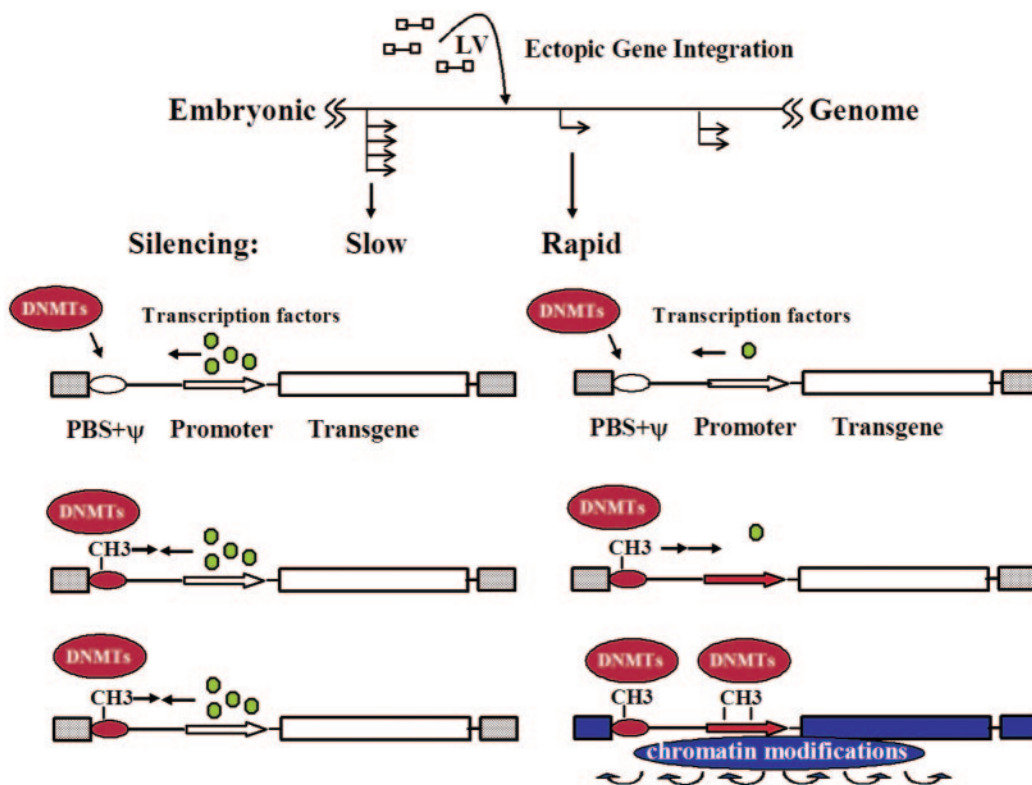


FIG. 9. Hypothesized ectopic transgene silencing model of embryonic cells. A stepwise DNA methylation and chromatin modification process is illustrated for the ectopic transgene in embryonic genomes. The first step involves de novo DNMTs, which starts from the PBS+ψ region in the provirus as a silencing initiation center; the CpG methylation then spreads to the surrounding DNA but may be counteracted by active transcription factors bound to the promoter region of nonsilenced loci. With increased CpG methylation and gradually decreased promoter activity, the transcription is silenced. The third step involves chromatin modifications that take place after DNA methylation, and this can further spread across the entire transgene loci. The condensed chromatin structure renders the transgene permanently silenced. Red area, methylated DNA; blue area, modified chromatin. Further details can be found in the Discussion.

to the heterochromatin pattern after transgene silencing. Interestingly, the H3 tail deacetylation was not restricted to the methylated DNA regions in the silenced cells but was detected in the entire provirus; however, in nonsilenced cells, the H3 tail was not modified although the PBS+ψ site was hypermethylated. Although the temporal relationship between DNA methylation and histone modifications has not been directly pinpointed, our results suggest that methylation in the internal promoter region, and chromatin modifications including H3 deacetylation and histone code switch across the entire proviral locus, are coupled with LV transgene silencing.

It is still controversial as to what triggers the initial event of transgene silencing (21, 32). Our comparative study of DNA methylation and H3 tail acetylation/deacetylation in silenced and nonsilenced cells from the same parental cell clone indicates that CpG methylation may not correlate with histone modifications. The methylation in the PBS+ψ region was independent of histone code changes because in nonsilenced cells it was quickly hypermethylated regardless of hyperacetylated H3 tail and active transcription. However, the kinetics of CpG methylation in the promoter region correlated well with the timing of transgene silencing. Therefore, methylation of the LV internal promoter is coupled with the initiation of transgene silencing, and followed by chromatin modifications across the entire provirus; further chromatin modifications

may render the methylated promoter silenced permanently and nonresponsive to DNMT inhibitors.

The silencing of ectopic transgenes in the EC cells is dynamic and may spread further into host genome. In the present study, we did not detect significant effects on flanking host cell genes located 45 to 50 kbp away from the integration site. Thus, the epigenetic modifications may not spread far beyond the integration loci, possibly due to the presence of certain boundary elements or insulators that can block the advance of the silencing machinery. Nevertheless, the analysis of one single-cell clone may not reflect general genome response after LV integration and silencing; large-scale host gene expression profiling will be necessary to decipher the global effects of LV integration and host response.

To summarize these results, a model describing the molecular events of LV silencing in the EC cells is presented (Fig. 9). After LV integration, the cellular methylation machinery rapidly initiates a de novo methylation process near the PBS+ψ region; the wave of DNA methylation may spread into the neighboring DNA. The methylated DNA has low affinity to transcription factors and diminished general transcriptional activity (4, 13). The high transcriptional activity of active promoters may counteract the effect of DNA methylation. It appears that the gradual down-regulated promoter activity, possibly initiated by chromatin and/or DNA alterations, triggers a wave of chromatin modifica-

tions, including histone tail deacetylation and histone code switch across the entire provirus, which induces chromatin condensation and leads to permanent transgene silencing.

Although oncoretroviral vectors are quickly silenced in both EC cells and preimplantation embryos (3, 27), HIV-1-based SIN LVs are relatively resistant to transgene silencing in preimplantation embryos (15, 24). It is conceivable that EC and ES cells may express differentiating factors that contribute differently to ectopic transgene silencing. Our study for the first time clearly demonstrates that DNA methylation and chromatin modifications are associated with LV transgene silencing. Whether the epigenetic mechanisms characterized here also exist in preimplantation embryos or other stem cell types awaits further exploration.

In summary, we demonstrate that a dynamic DNA methylation and chromatin modification process is associated with LV transgene silencing in EC cells. Further modifications of LVs, such as using boundary elements or insulators between PBS+ $\psi$  and the internal promoter region to prevent the spread of DNA methylation, may alleviate LV silencing and provide a long-term transgene expression solution in future stem cell studies. In addition, the evaluation of epigenetic chromatin modifications and the effects on host gene expression after provirus insertion can help resolve important safety issues in future LV gene therapy applications.

#### ACKNOWLEDGMENTS

We thank J. Bungert, X. D. Fu, and R. Brinster for helpful discussions and critical reading of the manuscript.

This study was sponsored by NIH grant HL59412.

#### REFERENCES

- Brooks, A. R., R. N. Harkins, P. Wang, H. S. Qian, P. Liu, and G. M. Rubanyi. 2004. Transcriptional silencing is associated with extensive methylation of the CMV promoter following adenoviral gene delivery to muscle. *J. Gene Med.* **6**:395–404.
- Challita, P. M., D. Skelton, A. El-Khoueiry, X. J. Yu, K. Weinberg, and D. B. Kohn. 1995. Multiple modifications in *cis* elements of the long terminal repeat of retroviral vectors lead to increased expression and decreased DNA methylation in embryonic carcinoma cells. *J. Virol.* **69**:748–755.
- Cherry, S. R., D. Biniszkiewicz, L. van Parijs, D. Baltimore, and R. Jaenisch. 2000. Retroviral expression in embryonic stem cells and hematopoietic stem cells. *Mol. Cell. Biol.* **20**:7419–7426.
- Deng, G., A. Chen, E. Pong, and Y. S. Kim. 2001. Methylation in hMLH1 promoter interferes with its binding to transcription factor CBF and inhibits gene expression. *Oncogene* **20**:7120–7127.
- Fox, A. H., Y. W. Lam, A. K. Leung, C. E. Lyon, J. Andersen, M. Mann, and A. I. Lamond. 2002. Paraspeckles: a novel nuclear domain. *Curr. Biol.* **12**:13–25.
- Gautsch, J. W., and M. C. Wilson. 1983. Delayed de novo methylation in teratocarcinoma suggests additional tissue-specific mechanisms for controlling gene expression. *Nature* **301**:32–37.
- Gropp, M., P. Itsykson, O. Singer, T. Ben-Hur, E. Reinhardt, E. Galun, and B. E. Reubinoff. 2003. Stable genetic modification of human embryonic stem cells by lentiviral vectors. *Mol. Ther.* **7**:281–287.
- Hawley, R. G. 2001. Progress toward vector design for hematopoietic stem cell gene therapy. *Curr. Gene Ther.* **1**:1–17.
- Hino, S., J. Fan, S. Taguwa, K. Akasaka, and M. Matsuoka. 2004. Sea urchin insulator protects lentiviral vector from silencing by maintaining active chromatin structure. *Gene Ther.* **11**:819–828.
- Imren, S., E. Payen, K. A. Westerman, R. Pawliuk, M. E. Fabry, C. J. Eaves, B. Cavilla, L. D. Wadsworth, Y. Beuzard, E. E. Bouhassira, R. Russell, I. M. London, R. L. Nagel, P. Leboulch, and R. K. Humphries. 2002. Permanent and panerythroid correction of murine beta thalassemia by multiple lentiviral integration in hematopoietic stem cells. *Proc. Natl. Acad. Sci. USA* **99**:14380–14385.
- Jahner, D., H. Stuhlmann, C. L. Stewart, K. Harbers, J. Lohler, I. Simon, and R. Jaenisch. 1982. De novo methylation and expression of retroviral genomes during mouse embryogenesis. *Nature* **298**:623–628.
- Krause, D. S., N. D. Theise, M. I. Collector, O. Henegariu, S. Hwang, R. Gardner, S. Neutzel, and S. J. Sharkis. 2001. Multi-organ, multi-lineage engraftment by a single bone marrow-derived stem cell. *Cell* **105**:369–377.
- Ku, J. L., S. B. Kang, Y. K. Shin, H. C. Kang, S. H. Hong, I. J. Kim, J. H. Shin, I. O. Han, and J. G. Park. 2004. Promoter hypermethylation down-regulates RUNX3 gene expression in colorectal cancer cell lines. *Oncogene* **23**:6736–6742.
- LaFace, D., P. Hermonat, E. Wakeland, and A. Peck. 1988. Gene transfer into hematopoietic progenitor cells mediated by an adeno-associated virus vector. *Virology* **162**:483–486.
- Lois, C., E. J. Hong, S. Pease, E. J. Brown, and D. Baltimore. 2002. Germline transmission and tissue-specific expression of transgenes delivered by lentiviral vectors. *Science* **295**:868–872.
- Ma, Y., A. Ramezani, R. Lewis, R. G. Hawley, and J. A. Thomson. 2003. High-level sustained transgene expression in human embryonic stem cells using lentiviral vectors. *Stem Cells* **21**:111–117.
- May, C., S. Rivella, A. Chadburn, and M. Sadelain. 2002. Successful treatment of murine beta-thalassemia intermedia by transfer of the human beta-globin gene. *Blood* **99**:1902–1908.
- McBurney, M. W. 1993. P19 embryonal carcinoma cells. *Int. J. Dev. Biol.* **37**:135–140.
- McBurney, M. W., E. M. Jones-Villeneuve, M. K. Edwards, and P. J. Anderson. 1982. Control of muscle and neuronal differentiation in a cultured embryonal carcinoma cell line. *Nature* **299**:165–167.
- Mummaneni, P., K. A. Walker, P. L. Bishop, and M. S. Turker. 1995. Epigenetic gene inactivation induced by a *cis*-acting methylation center. *J. Biol. Chem.* **270**:788–792.
- Mutskov, V., and G. Felsenfeld. 2004. Silencing of transgene transcription precedes methylation of promoter DNA and histone H3 lysine 9. *EMBO J.* **23**:138–149.
- Pannell, D., and J. Ellis. 2001. Silencing of gene expression: implications for design of retrovirus vectors. *Rev. Med. Virol.* **11**:205–217.
- Pawliuk, R., K. A. Westerman, M. E. Fabry, E. Payen, R. Tighe, E. E. Bouhassira, S. A. Acharya, J. Ellis, I. M. London, C. J. Eaves, R. K. Humphries, Y. Beuzard, R. L. Nagel, and P. Leboulch. 2001. Correction of sickle cell disease in transgenic mouse models by gene therapy. *Science* **294**:2368–2371.
- Pfeifer, A., M. Ikawa, Y. Dayn, and I. M. Verma. 2002. Transgenesis by lentiviral vectors: lack of gene silencing in mammalian embryonic stem cells and preimplantation embryos. *Proc. Natl. Acad. Sci. USA* **99**:2140–2145.
- Ramezani, A., T. S. Hawley, and R. G. Hawley. 2003. Performance- and safety-enhanced lentiviral vectors containing the human interferon-beta scaffold attachment region and the chicken beta-globin insulator. *Blood* **101**:4717–4724.
- Schroder, A., P. Shinn, H. Chen, C. Berry, J. Ecker, and F. Bushman. 2002. HIV-1 Integration in the human genome favors active genes and local hotspots. *Cell* **110**:521–529.
- Stuhlmann, H., D. Jahner, and R. Jaenisch. 1981. Infectivity and methylation of retroviral genomes is correlated with expression in the animal. *Cell* **26**:221–232.
- Turker, M. S. 2002. Gene silencing in mammalian cells and the spread of DNA methylation. *Oncogene* **21**:5388–5393.
- Turner, B. M. 2002. Cellular memory and the histone code. *Cell* **111**:285–291.
- Uchida, N., R. E. Sutton, A. M. Frieria, D. He, M. J. Reitsma, W. C. Chang, G. Veres, R. Scollay, and I. L. Weissman. 1998. HIV, but not murine leukemia virus, vectors mediate high efficiency gene transfer into freshly isolated G0/G1 human hematopoietic stem cells. *Proc. Natl. Acad. Sci. USA* **95**:11939–11944.
- Wilson, J. M., O. Danos, M. Grossman, D. H. Raulet, and R. C. Mulligan. 1990. Expression of human adenosine deaminase in mice reconstituted with retrovirus-transduced hematopoietic stem cells. *Proc. Natl. Acad. Sci. USA* **87**:439–443.
- Yao, S., T. Sukonnik, T. Kean, R. R. Bharadwaj, P. Pasceri, and J. Ellis. 2004. Retrovirus silencing, variegation, extinction, and memory are controlled by a dynamic interplay of multiple epigenetic modifications. *Mol. Ther.* **10**:27–36.
- Zaiss, A.-K., S. Son, and L.-J. Chang. 2002. RNA 3'-readthrough of oncoretrovirus and lentivirus: implications in vector safety and efficacy. *J. Virol.* **76**:7209–7219.